

# Barely fluorescent molecules. I. Twin-discharge jet laser-induced fluorescence spectroscopy of HSnCl and DSnCl

Cite as: J. Chem. Phys. **156**, 184307 (2022); <https://doi.org/10.1063/5.0090628>

Submitted: 08 March 2022 • Accepted: 20 April 2022 • Accepted Manuscript Online: 21 April 2022 •  
Published Online: 13 May 2022

Gretchen Rothschofp,  Tony C. Smith and  Dennis J. Clouthier



View Online



Export Citation



CrossMark

## ARTICLES YOU MAY BE INTERESTED IN

[Barely fluorescent molecules. II. Twin-discharge jet laser-induced fluorescence spectroscopy of HSnBr and DSnBr](#)

The Journal of Chemical Physics **156**, 184308 (2022); <https://doi.org/10.1063/5.0090629>

[Systematic bottom-up molecular coarse-graining via force and torque matching using anisotropic particles](#)

The Journal of Chemical Physics **156**, 184118 (2022); <https://doi.org/10.1063/5.0085006>

[Molecular vibrational imaging at nanoscale](#)

The Journal of Chemical Physics **156**, 160902 (2022); <https://doi.org/10.1063/5.0082747>

Lock-in Amplifiers  
up to 600 MHz



Zurich  
Instruments



# Barely fluorescent molecules. I. Twin-discharge jet laser-induced fluorescence spectroscopy of HSnCl and DSnCl

Cite as: J. Chem. Phys. 156, 184307 (2022); doi: 10.1063/5.0090628

Submitted: 8 March 2022 • Accepted: 20 April 2022 •

Published Online: 13 May 2022



View Online



Export Citation



CrossMark

Gretchen Rothschof, Tony C. Smith,  and Dennis J. Clouthier<sup>a)</sup> 

## AFFILIATIONS

Ideal Vacuum Products, LLC, 5910 Midway Park Blvd. NE, Albuquerque, New Mexico 87109, USA

<sup>a)</sup> Author to whom correspondence should be addressed: [djc@ideavac.com](mailto:djc@ideavac.com)

## ABSTRACT

The divalent tin transient molecules HSnCl and DSnCl have been detected for the first time by laser-induced fluorescence (LIF) spectroscopy. HSnCl/DSnCl were produced in a twin-discharge jet using separate precursor streams of SnH<sub>4</sub>/SnD<sub>4</sub> and the discharge products from HCl/DCl, both diluted in high pressure argon. The  $\tilde{A}^1A''-\tilde{X}^1A'$  spectrum of HSnCl consists of a single vibronic 0<sub>0</sub><sup>0</sup> band with a very short fluorescence lifetime (~30 ns). In contrast, the LIF spectrum of DSnCl exhibits three bands (0<sub>0</sub><sup>0</sup>, 2<sub>0</sub><sup>1</sup>, and 2<sub>0</sub><sup>2</sup>), whose fluorescence lifetimes decrease from 393 ns (0<sub>0</sub><sup>0</sup>) to less than 10 ns (2<sub>0</sub><sup>2</sup>). Single vibronic level emission spectra have been recorded, providing information on all three vibrational modes in the ground state. Previous detailed *ab initio* studies indicate that these molecules dissociate into SnCl + H on the excited state potential surface and this is the cause of the short fluorescence lifetimes and breaking off of the fluorescence. It is fortunate that the HSnCl excited state zero-point level is still fluorescent or it would not be detectable by LIF spectroscopy.

Published under an exclusive license by AIP Publishing. <https://doi.org/10.1063/5.0090628>

## I. INTRODUCTION

Building on our previous studies of the transient silicon- [monohalosilylenes (HSiX); X = F, Cl, Br, I] and germanium-containing [monohalogermynes (HGGeX); X = H, Cl, Br, I] triatomic molecules,<sup>1-14</sup> we have recently turned our attention to their tin analogs. Spectroscopic studies of tin-containing transient molecules are challenging due to their high reactivity, limited stability, paucity of viable precursors, and the complexities due to the ten naturally occurring tin isotopes. The electronic spectra of several gas phase diatomic molecules containing tin are known<sup>15</sup> (Sn<sub>2</sub>, SnH, SnO, SnS, SnSe, SnTe, SnF, SnCl, SnBr, and SnI) but there are very few accounts of the microwave, infrared, or electronic spectra of gas phase polyatomic tin species.

In 2018, we reported the spectroscopic detection and characterization of the tin dihydride molecule.<sup>16</sup> SnH<sub>2</sub> and SnD<sub>2</sub> were identified for the first time by laser-induced fluorescence (LIF) and emission spectroscopic techniques through the  $\tilde{A}^1B_1-\tilde{X}^1A_1$  electronic transition near 630 nm. These reactive species were prepared in a pulsed electric discharge jet using (CH<sub>3</sub>)<sub>4</sub>Sn or SnH<sub>4</sub>/SnD<sub>4</sub> precursors diluted in high pressure argon. Transitions to the electronic

excited state of the jet-cooled molecules were probed with LIF, and the ground state energy levels were measured from single rovibronic level emission spectra. The LIF spectrum of SnH<sub>2</sub> is very simple, consisting of only the 0<sub>0</sub><sup>0</sup>, 2<sub>0</sub><sup>1</sup>, 2<sub>0</sub><sup>2</sup> and possibly 2<sub>0</sub><sup>3</sup> cold bands, each of which comprises at most a few rotational lines.

The 0-0 band LIF spectrum of SnD<sub>2</sub> afforded just sufficient rotational structure to determine the ground and excited state geometries:  $r_0'' = 1.768$  Å,  $\theta_0'' = 91.0^\circ$ ,  $r_0' = 1.729$  Å, and  $\theta_0' = 122.9^\circ$ . All of the observed LIF bands show evidence of a rotational-level-dependent predissociation process, which rapidly decreases the fluorescence yield and lifetime with increasing rotational angular momentum in each excited vibronic level. This behavior is analogous to that observed in SiH<sub>2</sub> and GeH<sub>2</sub> and is suggested to lead to the formation of ground state tin atoms and hydrogen molecules.

The monostannyls (HSnX; X = F, Cl, Br, I) would have sufficiently large rotational constants that their LIF spectra could potentially be rotationally resolved, providing structural information, if they fluoresce and if they could be synthesized. Although the monohalosilylenes (HSiX; X = F, Cl, Br, I) and monohalogermynes (HGGeX; X = Cl, Br, I) are readily obtained in the gas phase by electric

discharge decomposition of the corresponding stable trihalosilanes ( $\text{HSiX}_3$ ) and trihalogermanes ( $\text{HGeX}_3$ ), the analogous trihalostannanes ( $\text{HSnX}_3$ ), which are largely unknown and unstable, are not viable precursors for the divalent monohalostannylenes ( $\text{HSnX}$ ). We theorized that the reactions of  $\text{SnH}_4$  and  $\text{HX}$  or their discharge products ( $\text{SnH}_2$ ,  $\text{X}$  atoms, etc.) had the potential to produce the  $\text{HSnX}$  species, but it would be necessary to keep the reactants apart until the moment of vacuum expansion as  $\text{SnH}_4$  is a very reactive and unstable species. The solution was to use a twin-discharge jet scheme, and this strategy has turned out to be quite successful as reported in the present study of  $\text{HSnCl}$  and  $\text{DSnCl}$ .

## II. EXPERIMENT

This work relies on our development of a twin-discharge jet, based largely on the dual-channel discharge nozzle reported in 1996 by Bezant *et al.*<sup>17</sup> These authors used one channel of their device to sputter metal atoms and the other to introduce a stable reactant (with or without discharge). The two gas streams mixed downstream, producing metal-containing transient species. In our implementation, the gas pulses from two independent pulsed molecular beam valves (General Valve, series 9) were expanded into the top of a Y-shaped circular channel (2 mm diameter) milled along the central axis of a black Delrin sandwich. Each leg of the Y is provided with a pair of metallic discharge electrodes, and the gas flows mix at the junction of the two channels before expanding into vacuum. The timings of the pulsed valve openings and closings and the firing of the discharges can be varied independent of each other to accommodate the flow characteristics of different feed gases. In the present instance, we used stainless steel electrodes as the aim was to produce fragments of the precursors rather than metal atoms from sputtering.

Our twin-discharge jet was tested using  $\text{F}_2$  in helium (excimer gas mixture of 0.088%  $\text{F}_2$  in helium) with the discharge on and disilane ( $\text{Si}_2\text{H}_6$ ) in argon with the discharge off. Observation of very strong LIF signals of monofluorosilylene ( $\text{HSiF}$ )<sup>1–3</sup> in the 23 000–24 500  $\text{cm}^{-1}$  region allowed us to optimize the experimental conditions, gas pressures, and delays to maximize the production of the transient molecule and the laser-induced fluorescence signals. Encouraged by this success, we immediately attempted to observe  $\text{HSnF}$  using stannane and fluorine precursors. Unstable  $\text{SnH}_4$  liquid (*vide infra*) was cooled in a Pyrex U-tube to  $-110^\circ\text{C}$  (ethanol/liquid  $\text{N}_2$  slush), pressurized with 55 psi of argon, and delivered to one of the pulsed valves in the twin-discharge apparatus. The  $\text{F}_2$  excimer gas mixture was delivered to the second pulsed valve through a regulator at various pressures. Despite considerable effort, no  $\text{HSnF}$  LIF signals were ever detected. This was reminiscent of previous studies in our laboratories in which we attempted to observe  $\text{HGeF}$  using a single discharge through  $\text{H}_3\text{GeF}$ , again without success.<sup>9</sup>

Fortunately, searches for the spectra of  $\text{HSnCl}$  and  $\text{DSnCl}$  were more successful.  $\text{SnH}_4$  and  $\text{SnD}_4$  were synthesized by the  $\text{LiAlH}_4$  or  $\text{LiAlD}_4$  reduction of  $\text{SnCl}_4$  as previously described.<sup>16</sup>  $\text{HCl}$  (Matheson) and  $\text{DCl}$  (Sigma-Aldrich) were used as received. The LIF spectra of  $\text{HSnCl}$  and  $\text{DSnCl}$  were produced in the twin-discharge jet under the following conditions:  $\text{SnH}_4$  or  $\text{SnD}_4$  liquid was cooled in a Pyrex U-tube to  $-110^\circ\text{C}$  (ethanol/liquid  $\text{N}_2$  slush) and pressurized with 55 psi of argon. One atmosphere of  $\text{HCl}$  or  $\text{DCl}$  gas was diluted with 400 psi of argon, and the mixture was delivered

to the second pulsed valve through a regulator at a pressure of 105 psi (gauge). Experiments showed that the best conditions were with an electric discharge in the  $\text{HCl}/\text{DCl}$  channel but no discharge in the stannane channel.

Two different tunable lasers were used to excite LIF in this experiment. For low resolution ( $2\text{--}5\text{ cm}^{-1}$ ) survey work, an optical parametric oscillator (OPO-A, GWU-Lasertechnik) pumped with the 355 nm output of a tripled neodymium:yttrium aluminum garnet (Nd:YAG) laser and scannable from 720–400 nm was employed. Moderate resolution ( $0.1\text{ cm}^{-1}$ ) spectra were recorded using a Nd:YAG pumped dye laser (Lumonics HD-500) excitation source. These spectra were calibrated with optogalvanic lines from various argon- and neon-filled hollow cathode lamps to an estimated absolute accuracy of  $0.1\text{ cm}^{-1}$ .

The reactive intermediates were rotationally and vibrationally cooled by free jet expansion into vacuum at the exit of the twin-discharge jet apparatus. The fluorescence was collected by a lens, focused through appropriate longwave pass filters and onto the photocathode of a photomultiplier tube (RCA C31034A). The LIF and calibration spectra were digitized and recorded simultaneously on a homebuilt computerized data acquisition system.

For emission spectroscopy, previously measured LIF band maxima in the spectra of  $\text{HSnCl}$  or  $\text{DSnCl}$  were excited by the Lumonics dye laser and the resulting fluorescence was collected with an  $f/0.7$  aspheric lens and imaged with  $f/4$  optics onto the entrance slit of a 0.5 m scanning monochromator (Spex 500M). The pulsed fluorescence signals were detected with a gated CCD camera (Andor iStar 320T) and recorded digitally. The emission spectra were calibrated to an estimated accuracy of  $1\text{ cm}^{-1}$  using emission lines from an argon hollow cathode lamp. A 1200 line/mm grating blazed at 750 nm was employed in this work, which gave a bandpass of 29.9 nm with an 18 mm effective active area on the CCD. A spectral resolution of 0.02 nm was typical depending on the signal intensity.

Fluorescence lifetimes were measured by summation averaging 500 fluorescence decay curves employing a Tektronix TDS-3054 oscilloscope with the excitation laser tuned to a specific LIF Q-branch. The laser was then slightly detuned from the LIF line, a second background sum was recorded, and it was subtracted from the fluorescence decay curve to remove the scattered laser light and discharge glow contributions. The resulting data were plotted as the natural logarithm of the fluorescence intensity vs time, and the linear portion of the decay was least squares fitted to a linear function to obtain the fluorescence lifetime and statistical error.

## III. SUMMARY OF CONTEMPORANEOUS *AB INITIO* STUDY

Concurrent with the present experimental effort, Tarroni and Clouthier<sup>18</sup> embarked on an extensive *ab initio* study to predict which of the triatomic halosilylenes, halogermynes, and halostannylenes ( $\text{HMx}$ ;  $\text{M} = \text{Si}, \text{Ge}, \text{Sn}$ ;  $\text{X} = \text{F}, \text{Cl}, \text{Br}, \text{I}$ ) would fluoresce or phosphoresce and why. The authors found that the  $\tilde{a}^3A''$  states of all these molecules have deep bonding wells and would be expected to exhibit extensive laser-induced phosphorescence (LIP) spectra. These spectra would be at quite low energies for the  $\text{HSiX}$  species [732 nm ( $\text{HSiF}$ ) to 908 nm ( $\text{HSiI}$ )] and are probably undetectably weak. The LIP spectra of the germanium- and tin-containing molecules may be experimentally observable as they are

shifted to higher energies (1000–2000  $\text{cm}^{-1}$ ) and would be expected to be stronger due to greater spin-orbit coupling. In contrast, the depth of the bonding wells of the  $\tilde{A}^1A''$  states of HMX varies substantially depending on M and X with dissociation leading to the production of  $\text{H}(^2S) + \text{MX}(^2\Pi)$  as the primary factor controlling fluorescence. The results indicated that the HSiX and most of the HGeX molecules should fluoresce, in agreement with our published reports.<sup>1–12</sup> The calculations predicted that HGeF and HSnF, species whose LIF spectra we have been unable to detect, would be non-fluorescent due to dissociation from the excited state zero-point level.

For HSnCl, the *ab initio* results were very interesting as they indicated the opening of the dissociation channel only slightly above the  $\tilde{A}$  state vibrational zero-point level, extending to two or three quanta of the bending mode in DSnCl. Thus, theory predicts that HSnCl and DSnCl, if they can be generated in the gas phase, should be barely fluorescent molecules, with spectra of limited extent and short fluorescence lifetimes.

## IV. RESULTS

### A. LIF spectra

A search for the spectrum of HSnCl using our tunable OPO source gave the results illustrated in Fig. 1. Two traces are shown: the upper trace (short decay) is the spectrum obtained by gating the LIF signal for 100 ns delayed 20 ns after the laser pulse, and the bottom trace (long decay) is that recorded with a 2  $\mu\text{s}$  wide gate delayed 1  $\mu\text{s}$  after the laser. The short-lived bands between 20 000 and 20 500  $\text{cm}^{-1}$  were readily identified as due to diatomic tin,<sup>19</sup> and the long decay bands are from the A–X band system of SnCl<sup>20</sup> with an

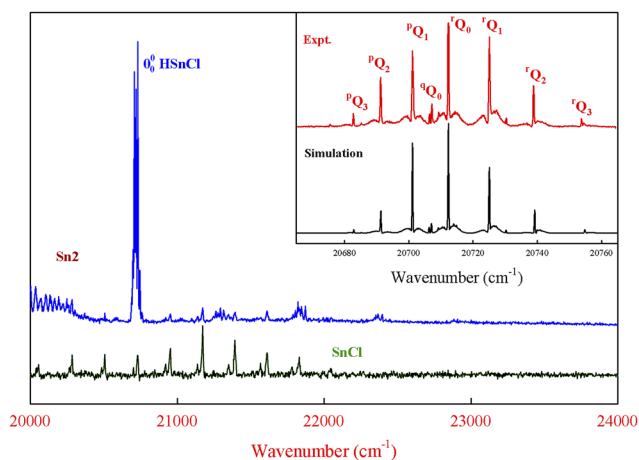


**FIG. 1.** The low resolution (3–5  $\text{cm}^{-1}$ ) LIF spectrum obtained in a twin-jet discharge with  $\text{SnH}_4 + \text{argon}$  in one jet (discharge off) and  $\text{HCl} + \text{argon}$  (discharge on) in the other. The upper trace (short delay spectrum) is that obtained with a gated integrator gate width of 100 ns, delayed 20 ns after the laser pulse. The bottom trace (long delay spectrum) is that obtained with a gated integrator gate width of 2  $\mu\text{s}$ , delayed 1  $\mu\text{s}$  after the laser pulse. The inset shows a medium resolution (0.1  $\text{cm}^{-1}$ ) LIF spectrum of the 0–0 band of HSnCl and the corresponding simulation ( $\text{H}^{120}\text{Sn}^{35}\text{Cl}$ , 0.25  $\text{cm}^{-1}$  FWHM, 20 K rotational temperature) of the band based on the *ab initio* geometries.<sup>18</sup>

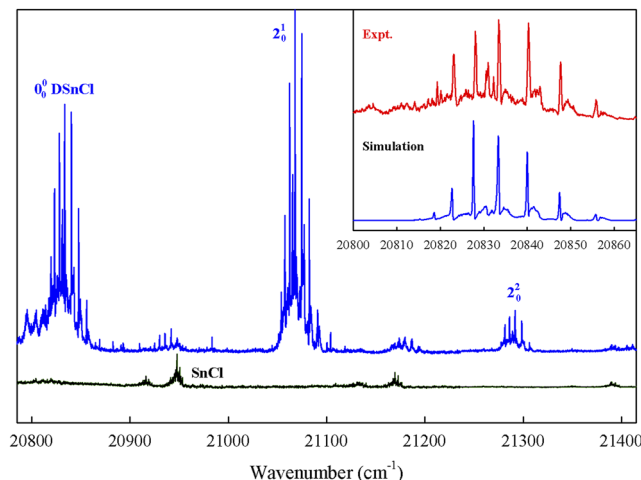


**FIG. 2.** The medium resolution (0.1  $\text{cm}^{-1}$ ) LIF spectrum obtained in a twin-jet discharge with  $\text{SnD}_4 + \text{argon}$  in one jet (discharge off) and  $\text{DCl} + \text{argon}$  (discharge on) in the other. The upper trace is the short delay spectrum (see Fig. 1), and the long delay spectrum is shown in the bottom trace. The inset shows a medium resolution (0.1  $\text{cm}^{-1}$ ) LIF spectrum of the 0–0 band of DSnCl and the corresponding simulation ( $\text{D}^{120}\text{Sn}^{35}\text{Cl}$ , 0.25  $\text{cm}^{-1}$  FWHM, 15 K rotational temperature) of the band based on the *ab initio* geometries.<sup>18</sup>

obvious chlorine isotope splitting. In addition, the short decay spectrum exhibits a very strong band centered at  $\sim 20\,715\text{ cm}^{-1}$  with clear subband structure even at this low resolution.

Using the Lumonics dye laser, we obtained the medium resolution spectrum of the strong band, as illustrated in the inset of Fig. 1. This is clearly a perpendicular band of an asymmetric top. There are obvious axis-switching Q-branches, which would be expected for a species of low-symmetry ( $C_s$  or lower), and our simulation of the spectrum (*c*-type selection rules) from the *ab initio* geometries<sup>18</sup> (inset of Fig. 1) matches so well there can be little doubt this is the LIF spectrum of HSnCl. We assign the strong, short-lived LIF feature in Fig. 1 as the  $0_0^0$  band of the  $\tilde{A}^1A'' - \tilde{X}^1A'$  electronic transition of the HSnCl transient molecule.

Twin-discharge jet spectroscopy with  $\text{SnD}_4$  and  $\text{DCl}$  produced the medium resolution DSnCl LIF spectrum shown in Fig. 2. We label the vibrations conventionally as  $\nu_1 = \text{Sn-H stretch}$ ,  $\nu_2 = \text{bend}$ , and  $\nu_3 = \text{Sn-Cl stretch}$ . The deuterium isotope shift of the 0–0 band is 124.3  $\text{cm}^{-1}$ , very comparable to the *ab initio* value of 126  $\text{cm}^{-1}$ , and the *ab initio* simulation of the band (inset of Fig. 2) agrees very well. The DSnCl LIF spectrum is more extensive than that of HSnCl, as predicted in the *ab initio* study,<sup>18</sup> due to the lower zero-point energy of the deuterated species. The bending vibrational interval identified in the DSnCl spectrum is  $\nu_2' = 234.3\text{ cm}^{-1}$  (*ab initio* = 247  $\text{cm}^{-1}$ ).<sup>18</sup> The positions and assignments of the observed LIF bands of HSnCl and DSnCl are summarized in Table I.

### B. Emission spectra

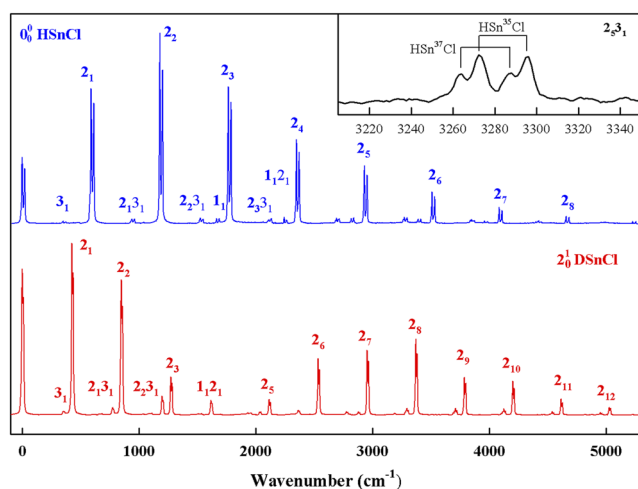
Single vibronic level (SVL) emission spectra of HSnCl and DSnCl were obtained by pumping the strong  ${}^1Q_0$  branches of the various bands. This transition populates the upper state  $K_a = 1$  levels, and the selection rules mandate that emission transitions can

**TABLE I.** Assignments and  ${}^rQ_0$  branch maxima of the observed bands ( $\text{cm}^{-1}$ ) in the LIF spectra of HSnCl and DSnCl. *Ab initio* values are given in square brackets.<sup>18</sup>

Assign.	HSnCl	DSnCl	Comment
$0_0^0$	20 706.3 [21 198]	20 830.6 [21 324]	D–H = 124.3 [126]
$2_0^1$	...	21 064.9	$\nu_2' = 234.3$ [247]
$2_0^2 3_1^0$	...	20 932.6	$2_0^2 - 356$
$2_0^2$	...	21 288.8	$2_0^1 + 223.9$

then occur down to ground state levels with  $K_a'' = 2$  and 0, producing resolvable doublets in the spectra, as shown by the examples in Fig. 3. The spectra are dominated by an extensive bending progression ( $\nu_2''$ ) with weaker bands due to the involvement of the Sn–H stretch ( $\nu_1''$ ) and the Sn–Cl stretch ( $\nu_3''$ ), giving vibrational fundamentals of  $\nu_1'' = 1665$ ,  $\nu_2'' = 591$ , and  $\nu_3'' = 349 \text{ cm}^{-1}$ . In the HSnCl 0–0 band emission spectrum, the bands in the  $2_n 3_1$  progression get progressively more complicated as  $n$  increases, which we assign as an increasing chlorine isotope splitting. The inset in Fig. 3 shows this effect for the  $2_5 3_1$  band. In contrast, the  $2_n$  and  $1_{1,2n}$  bands do not exhibit more complex rotational contours with increasing  $n$ , as expected for vibrational levels that do not involve the Sn–Cl stretch.

The bottom trace in Fig. 3 shows the emission spectrum obtained from laser excitation of the  ${}^rQ_0$  branch of the  $2_0^1$  band of DSnCl. This band system shows a radically different Franck–Condon profile with a node at  $2_4^1$  and no evidence of a transition to the  $1_1$  level. As in HSnCl, there is a  $2_n 3_1$  progression of bands, which show a prominent chlorine isotope effect, although these bands fall much closer to the bending progression. The  $1_{1,2n}$  progression was less prominent and more difficult to assign in

**FIG. 3.** Example emission spectra of HSnCl (top trace,  $0_0^0$  band  ${}^rQ_0$  excitation) and DSnCl (bottom trace,  $2_0^1$  band  ${}^rQ_0$  excitation) with some assignments. The inset shows the  $2_5^0 3_1^0$  emission band of HSnCl showing resolved  ${}^{35}\text{Cl}$  and  ${}^{37}\text{Cl}$  features. In each case, the abscissa is the wavenumber displacement from the excitation laser, giving a direct measure of the ground state vibrational energy.**TABLE II.** Vibrational levels of the  $\tilde{X}^1A'$  state of HSnCl and DSnCl (in  $\text{cm}^{-1}$  relative to the  $0_0$  level).

Assignment	HSn <sup>35</sup> Cl		DSn <sup>35</sup> Cl	
	Energy	Comment	Energy	Comment
$3_1$	349	$\nu_3'' = 349$	352	$\nu_3'' = 352$
$2_1$	591	$\nu_2'' = 591$	426	$\nu_2'' = 426$
$2_1 3_1$	940	$2_1 + 349$	776	$2_1 + 350$
$2_2$	1179	$2_1 + 588$	850	$2_1 + 424$
$2_2 3_1$	1521 and 1526 <sup>a</sup>	$2_2 + 347$	1198	$2_2 + 348$
$1_1$	1665	$\nu_1'' = 1665$	...	
$2_3$	1765	$2_2 + 586$	1273	$2_2 + 423$
$2_3 3_1$	2103 and 2112	$2_3 + 347$	1621	$2_3 + 348$
$1_{1,2_1}$	2244	$2_1 + 1653$	...	
$2_4$	2349	$2_3 + 584$	1696	$2_3 + 423$
$2_4 3_1$	2684 and 2692	$2_4 + 343$	2036 and 2042 <sup>a</sup>	$2_4 + 346$
$1_{1,2_2}$	2818	$2_2 + 1639$	...	
$2_5$	2930	$2_4 + 581$	2117	$2_4 + 421$
$2_5 3_1$	3264 and 3272	$2_5 + 342$	2452 and 2461	$2_5 + 344$
$1_{1,2_3}$	3390	$2_3 + 1625$	2363	$2_3 + 1090$
$2_6$	3509	$2_5 + 579$	2537	$2_5 + 420$
$2_6 3_1$	~3848 <sup>b</sup>	$2_6 + 339$	2869 and 2878	$2_6 + 341$
$1_{1,2_4}$	3959	$2_4 + 1610$	2776	$2363 + 413$
$2_7$	4085	$2_6 + 576$	2955	$2_6 + 418$
$2_7 3_1$	~4421 <sup>b</sup>	$2_7 + 336$	3281 and 3297	$2_7 + 342$
$1_{1,2_5}$	4527	$2_5 + 1597$	3186	$2776 + 410$
$2_8$	4658	$2_7 + 573$	3372	$2_7 + 417$
$2_8 3_1$	~4993 <sup>b</sup>	$2_8 + 335$	3690 and 3712	$2_8 + 340$
$1_{1,2_6}$	...	...	3595	$3186 + 409$
$2_9$	5229	$2_8 + 571$	3789	$2_8 + 417$
$1_{1,2_7}$			4005	$3595 + 410$
$2_9 3_1$			4128	$2_9 + 339$
$2_{10}$			4204	$2_9 + 415$
$1_{1,2_8}$			4413	$4005 + 408$
$2_{10} 3_1$			4539	$2_{10} + 335$
$2_{11}$			4616	$2_{10} + 412$
$1_{1,2_9}$			4818	$4413 + 405$
$2_{11} 3_1$			4952	$2_{11} + 336$
$2_{12}$			5028	$2_{11} + 412$
$1_{1,2_{10}}$			5221	$4818 + 403$
$2_{12} 3_1$			5362	$2_{12} + 334$
$2_{13}$			5437	$2_{12} + 409$
$1_{1,2_{11}}$			5624	$5221 + 403$
$2_{13} 3_1$			5770	$2_{13} + 333$
$2_{14}$			5847	$2_{13} + 410$
$1_{1,2_{12}}$			6026	$5624 + 402$
$2_{14} 3_1$			6177	$2_{14} + 330$
$2_{15}$			6252	$2_{14} + 405$
$1_{1,2_{13}}$			6427	$6026 + 401$
$2_{15} 3_1$			6582	$2_{15} + 330$
$2_{16}$			6658	$2_{15} + 406$

<sup>a</sup>When there are two entries, the first is for HSn<sup>37</sup>Cl and the second is for HSn<sup>35</sup>Cl.<sup>b</sup>The contours of these bands are complicated, making it difficult to assign the Cl isotope splittings.

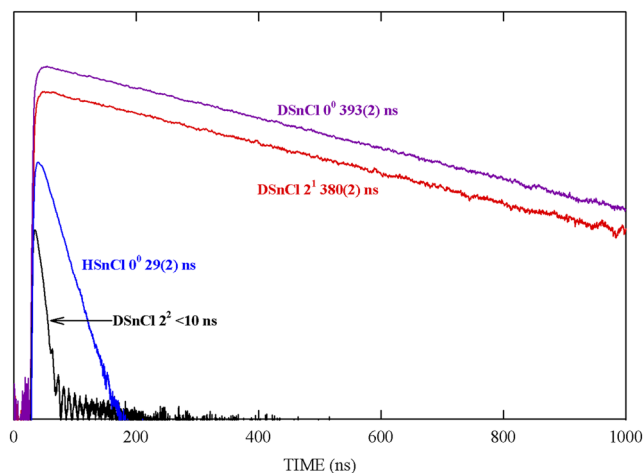


**FIG. 4.** Example fluorescence decays for various excited state vibronic levels of HSnCl and DSnCl. In each case, the dye laser (10 ns pulse width) excited a group of excited state  $K_a = 1$  levels ( $^1Q_0$  branch) and the subsequent fluorescence was monitored as a function of time. The decays were plotted as  $I_n$  (Intensity) vs time, and the linear portion was fitted to obtain the fluorescence lifetime in nanoseconds. The errors are estimated based on the variability of duplicate determinations.

DSnCl, but a series of such bands without detectable chlorine isotope effects was found in the  $0_0^0$  and  $2_0^1$  band spectra. The DSnCl vibrational fundamentals are  $\nu_1'' \sim 1090$  ( $1_1 2_3-2_3$  interval),  $\nu_2'' = 426$ , and  $\nu_3'' = 352$   $\text{cm}^{-1}$ , which exhibit the expected large deuterium effect on  $\nu_1''$ , moderate effect on  $\nu_2''$ , and almost negligible influence on  $\nu_3''$ . The measured ground state energy levels and assignments for HSnCl and DSnCl are presented in Table II.

### C. Fluorescence lifetimes

Fluorescence lifetimes were measured by laser excitation of a variety of Q-branches in the observed LIF bands. In general, the traces were reasonably good single exponential decays over two or more lifetimes, with some deviations at the beginning, due to imperfectly subtracted scattered light contributions and, at the end, due to inherent noise on the weaker signal. Some examples of the observed fluorescence decay curves are shown in Fig. 4, which also summarizes the results. Generally, we found little measurable variation in the lifetimes across the various Q-branches with a mean value for the HSnCl  $0^0$  vibronic state of  $29 \pm 2$  ns. The  $0^0$  level of DSnCl is much longer lived with a fluorescence lifetime of  $393 \pm 2$  ns, decreasing very slightly to  $380 \pm 2$  ns for  $2^1$  and then abruptly plummeting to less than 10 ns (this decay is comparable to the duration of the laser excitation pulse) for  $2^2$ . Clearly, as the DSnCl excited state energy increases to two quanta of the bending mode, the fluorescence lifetimes decrease abruptly, entirely consistent with the prediction<sup>18</sup> of the opening of a dissociative energy channel at low vibrational energies in the excited state.

## V. DISCUSSION

### A. The molecular structure of HSnCl

In the absence of rotationally resolved spectra, which would necessitate pure tin isotopes and/or very high resolution, we must

rely on theory to provide structural data for monochlorostannylene. The calculated ground and excited state  $\text{H}^{120}\text{Sn}^{35}\text{Cl}$   $r_e$  values are  $r''(\text{SnH}) = 1.794$  Å,  $r''(\text{SnCl}) = 2.381$  Å,  $\theta''(\text{HSnCl}) = 92.9^\circ$ ,  $r'(\text{SnH}) = 1.832$  Å,  $r'(\text{SnCl}) = 2.364$  Å, and  $\theta'(\text{HSnCl}) = 112.2^\circ$ . For comparison, the simple sum of the HSnCl single bond covalent radii<sup>21</sup> yields  $r(\text{SnH}) = 1.72$  Å and  $r(\text{SnCl}) = 2.39$  Å. The ground state SnH bond length is only slightly longer than that of  $\text{SnH}_2$  (1.768 Å)<sup>16</sup> and comparable to the ground state bond length of the SnH diatomic molecule (1.781 Å).<sup>15</sup> Similarly, the bond length of diatomic SnCl ( $X^2\Pi$ )<sup>22</sup> is 2.362 Å, only 0.019 Å shorter than in HSnCl. The  $92.9^\circ$  bond angle is slightly larger than that of  $\text{SnH}_2$  ( $91.0^\circ$ ) and follows the trend of decreasing calculated bond angle in HSiCl ( $95.0^\circ$ ) and HGeCl ( $93.8^\circ$ ).<sup>18</sup>

The changes in HSnCl structural parameters on  $\bar{A}^1A''-\bar{X}^1A'$  electronic excitation follow those found experimentally for HSiCl and HGeCl with a small increase in the M–H bond length, a small decrease in the M–Cl length, and a  $19.2^\circ$  (HGeCl)– $21.5^\circ$  (HSiCl) increase in the bond angle.<sup>18</sup> The above comparisons with similar molecules and the good agreement between calculated (*ab initio* rotational constants) and experimental HSnCl and DSnCl 0–0 band contours (Figs. 1 and 2) strongly suggest that the theoretical molecular structures of monochlorostannylene are quite realistic.

### B. Vibrational analysis

The ground state intervals obtained from the emission spectra were fitted to the standard anharmonic expansion of the following form:<sup>23</sup>

$$G_0(\nu) = \sum_{i=1}^3 \omega_i^0 \nu_i + \sum_{i=1}^3 \sum_{j \geq i}^3 x_{ij}^0 \nu_i \nu_j. \quad (1)$$

The resulting constants are presented in Table III, where it is evident that only a few of the anharmonicity constants were determinable, so the harmonic frequencies could not be obtained from this dataset. The Teller–Redlich product rule<sup>23</sup> mandates that

$$\frac{\omega_1^* \omega_2^* \omega_3^*}{\omega_1 \omega_2 \omega_3} \sqrt{\left(\frac{C}{C^*}\right) \left(\frac{M^*}{M}\right)^2 \left(\frac{m_H}{m_D}\right)^2}, \quad (2)$$

where an asterisk denotes DSnCl, the  $\omega$ 's are the harmonic frequencies,  $C$  is the rotational constant for the largest moment of inertia,  $M$  is the total molecular mass, and  $m_H$  and  $m_D$  are the masses of the hydrogen and deuterium atoms, respectively. In the absence of

**TABLE III.** Vibrational constants for the  $\bar{X}^1A'$  states of HSnCl and DSnCl (in  $\text{cm}^{-1}$ ).

Constant	HSnCl	DSnCl
$\omega_1^0$	1665.76(53)	1117.96(92)
$\omega_2^0$	592.43(15)	426.915(90)
$\omega_3^0$	350.25(48)	350.68(55)
$x_{11}^0$	...	...
$x_{22}^0$	−1.273(20)	−0.669(70)
$x_{33}^0$	...	...
$x_{12}^0$	−13.86(18)	−9.86(10)
$x_{13}^0$	...	...
$x_{23}^0$	−1.86(10)	−1.372(64)

proper harmonic frequencies, we have used the  $\omega_i^0$  values (Table III), which give a LHS ratio of 0.484 and a RHS ratio (using the *ab initio* rotational constants and the  $^{120}\text{Sn}$  and  $^{35}\text{Cl}$  isotopes) of 0.514. Given that the experimental frequencies include contributions from the various Sn and Cl isotopes and anharmonicities, the agreement is reasonable.

It is of interest to compare the derived HSnCl vibrational frequencies (Table III) to those of similar molecules. The  $\omega_i^0$  frequencies [HSnCl/DSnCl] of  $1666/1118\text{ cm}^{-1}$  are only slightly smaller than the corresponding ground state stretching fundamentals of  $\text{SnH}_2/\text{SnD}_2 = 1679/1204\text{ cm}^{-1}$ , suggesting that substitution of hydrogen with chlorine does not substantially affect the Sn–H stretch.<sup>16</sup> The Sn–Cl stretching frequencies are HSnCl = 350 and DSnCl = 351  $\text{cm}^{-1}$ , essentially unaffected by deuteration, and virtually identical to the diatomic SnCl frequency of  $353.6\text{ cm}^{-1}$ .<sup>20</sup>

As a further test of the validity of our identification of the spectra as due to HSnCl, we have generated Franck–Condon (FC) simulations of the SVL emission spectra, based solely on *ab initio* data. The simulation program, originally developed by Yang *et al.*<sup>24</sup> and locally modified for the calculation of SVL emission spectra, requires input of the molecular structures, vibrational frequencies, and mass-weighted Cartesian displacement coordinates from the force fields of the two combining states. Franck–Condon factors are then calculated in the harmonic approximation using the exact recursion relationships of Doctorov *et al.*<sup>25</sup> For both states, the geometry was optimized and the vibrational frequencies and normal coordinates were calculated using density functional theory (B3LYP) and aug-cc-pVTZ basis sets (aug-cc-pVTZ-PP with effective core potential for tin). The 0–0 band  $^PQ_1$  emission spectrum, in which each vibronic band consists of a single  $K'_a = 0 - K''_a = 1$  subband, is shown in Fig. 5. The corresponding FC simulation matches the strong bending mode ( $2_n$ ) progression and weak bend–SnCl stretch ( $2_n, 3_1$ ) combinations very well, buttressing our identification of the carrier of the spectra. The simulation overestimates the intensity of bands involving  $\nu''_1$ , as is found for simulations of the emission spectra of the halosilylenes<sup>3,5</sup> and halogermynes,<sup>10,11</sup> and is due to

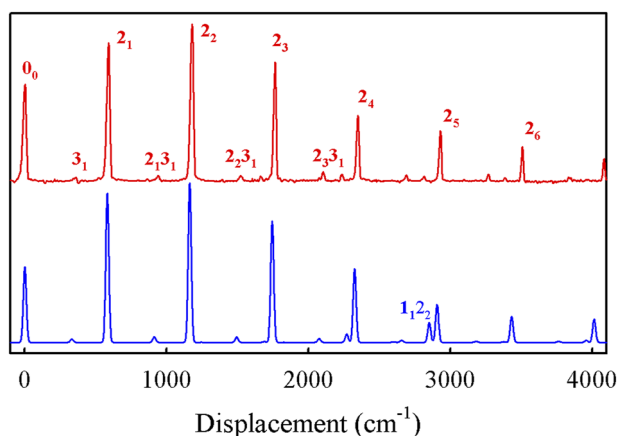


**FIG. 5.** Top: the SVL emission spectrum obtained by laser excitation of the  $^PQ_1$  branch of the 0–0 band of HSnCl with vibrational assignments. Bottom: the Franck–Condon simulation of the 0–0 band emission spectrum of  $\text{H}^{120}\text{Sn}^{35}\text{Cl}$  from *ab initio* data (see the text).

the neglect of the substantial  $\nu_1$  anharmonicity. More sophisticated calculations that explicitly include anharmonicity correct for these deficiencies.<sup>26–28</sup>

### C. Comparison to previous *ab initio* calculations

It is gratifying that the present experimental observations so closely follow the *ab initio* predictions of Tarroni and Clouthier.<sup>18</sup> The ground state fundamental frequencies are sensibly  $2\text{--}22\text{ cm}^{-1}$  smaller than the theoretical values for both isotopologues. The  $\tilde{A}\text{--}\tilde{X}$  theoretical  $T_0$  values are  $492/493\text{ cm}^{-1}$  higher than experiment, precisely the same trend as seen for the HGEX species, where there are more complete experimental data. Such systematic deviations are likely due to the use of pseudopotentials for the Ge and Sn atoms as well as the finite size of the basis sets and intrinsic limitations of the electron correlation treatment. Of more importance is the fact that the calculations predict that HSnCl dissociates into  $\text{H} + \text{SnCl}$  very low down in the  $\tilde{A}$  state potential, so that fluorescence should only be observed from the  $0^0$  and possibly  $2^1$  levels. In fact, we only see LIF from the zero-point level with a short fluorescence lifetime of  $29 \pm 2\text{ ns}$ . Deuterium substitution extends the LIF spectrum out to  $2_0^2$ , exactly as predicted by the calculations, simply as a result of the lower zero-point energy of DSnCl. As expected, the  $0^0$  and  $2^1$  levels of DSnCl have much longer fluorescence lifetimes (393 and 380 ns), decreasing dramatically to  $<10\text{ ns}$  for  $2^2$ , signaling the onset of dissociation. It is clearly evident that it is this dissociative process in the  $\tilde{A}^1A''$  state that makes HSnF nonfluorescent and HSnCl a barely fluorescent molecule.

## VI. CONCLUSIONS

The transient molecules HSnCl and DSnCl have been identified and characterized in the gas phase for the first time. These new species were “synthesized” in a twin-discharge jet in which  $\text{SnH}_4/\text{SnD}_4$  was reacted with the products of a HCl/DCl discharge. The wavenumbers of the observed LIF bands, the ground and excited state vibrational frequencies, the rotational band contours, the effects of deuterium substitution, and the breaking off of fluorescence at low excited state energies all coincide with *ab initio* predictions, providing incontrovertible evidence for the identities of the species detected. We have shown that HSnF is nonfluorescent under experimental conditions where HSiF is readily detected and that HSnCl is barely fluorescent, exhibiting only a single band in the LIF spectrum. Both of these observations are consistent with the *ab initio* predictions of Tarroni and Clouthier,<sup>18</sup> which indicate that these molecules dissociate ( $\text{HSnX} \rightarrow \text{H} + \text{MX}$ ) at very low vibrational energies in the  $\tilde{A}^1A''$  excited state.

## ACKNOWLEDGMENTS

This research was funded by Ideal Vacuum Products.

## AUTHOR DECLARATIONS

### Conflict of Interest

The authors have no conflicts to disclose.

## Author Contributions

All authors contributed equally to this work.

## DATA AVAILABILITY

The data that support the findings of this study are available within the article.

## REFERENCES

- <sup>1</sup>W. W. Harper, J. Karolczak, D. J. Clouthier, and S. C. Ross, *J. Chem. Phys.* **103**, 883 (1995).
- <sup>2</sup>W. W. Harper, D. A. Hostutler, and D. J. Clouthier, *J. Chem. Phys.* **106**, 4367 (1997).
- <sup>3</sup>D. A. Hostutler, D. J. Clouthier, and R. H. Judge, *J. Chem. Phys.* **114**, 10728 (2001).
- <sup>4</sup>W. W. Harper and D. J. Clouthier, *J. Chem. Phys.* **106**, 9461 (1997).
- <sup>5</sup>D. A. Hostutler, N. Ndiege, D. J. Clouthier, and S. W. Pauls, *J. Chem. Phys.* **115**, 5485 (2001).
- <sup>6</sup>H. Harjanto, W. W. Harper, and D. J. Clouthier, *J. Chem. Phys.* **105**, 10189 (1996).
- <sup>7</sup>D. J. Clouthier, W. W. Harper, C. M. Klusek, and T. C. Smith, *J. Chem. Phys.* **109**, 7827 (1998).
- <sup>8</sup>B. S. Tackett and D. J. Clouthier, *J. Chem. Phys.* **118**, 2612 (2003).
- <sup>9</sup>W. W. Harper and D. J. Clouthier, *J. Chem. Phys.* **108**, 416 (1998).
- <sup>10</sup>B. S. Tackett, D. J. Clouthier, K. L. Pacheco, and G. A. Schick, *J. Chem. Phys.* **124**, 124320 (2006).
- <sup>11</sup>B. S. Tackett, Y. Li, D. J. Clouthier, K. L. Pacheco, G. A. Schick, and R. H. Judge, *J. Chem. Phys.* **125**, 114301 (2006).
- <sup>12</sup>W. W. Harper, C. M. Klusek, and D. J. Clouthier, *J. Chem. Phys.* **109**, 9300 (1998).
- <sup>13</sup>J. Karolczak, W. W. Harper, R. S. Grev, and D. J. Clouthier, *J. Chem. Phys.* **103**, 2839 (1995).
- <sup>14</sup>T. C. Smith, D. J. Clouthier, W. Sha, and A. G. Adam, *J. Chem. Phys.* **113**, 9567 (2000).
- <sup>15</sup>K. P. Huber and G. Herzberg, "Constants of diatomic molecules," in *NIST Chemistry WebBook*, NIST Standard Reference Database Number 69, edited by P. J. Linstrom and W. G. Mallard, National Institute of Standards and Technology, Gaithersburg, MD, 2020, retrieved April 2, 2020, data prepared by J. W. Gallagher and R. D. Johnson III.
- <sup>16</sup>T. C. Smith and D. J. Clouthier, *J. Chem. Phys.* **148**, 024302 (2018).
- <sup>17</sup>A. J. Bezzant, D. D. Turner, G. Dormer, and A. M. Ellis, *J. Chem. Soc., Faraday Trans.* **92**, 3023 (1996).
- <sup>18</sup>R. Tarroni and D. J. Clouthier, *J. Chem. Phys.* **156**, 064304 (2022).
- <sup>19</sup>V. E. Bondybey, M. Heaven, and T. A. Miller, *J. Chem. Phys.* **78**, 3593 (1983).
- <sup>20</sup>A. Chatalic, D. Iacocca, and G. Pannetier, *J. Chim. Phys.* **70**, 908 (1973).
- <sup>21</sup>W. Gordy and R. L. Cook, *Microwave Molecular Spectra, Techniques of Chemistry* (Wiley, New York, 1984), Vol. XVIII.
- <sup>22</sup>G. S. Grubbs II, D. J. Frohman, S. E. Novick, and S. A. Cooke, *J. Mol. Spectrosc.* **280**, 85 (2012).
- <sup>23</sup>G. Herzberg, *Molecular Spectra and Molecular Structure. II. Infrared and Raman Spectra of Polyatomic Molecules* (Van Nostrand, New York, 1945).
- <sup>24</sup>D. S. Yang, M. Z. Zgierski, A. Bércecs, P. A. Hackett, P. N. Roy, A. Martinez, T. Carrington, Jr., D. R. Salahub, R. Fournier, T. Pang, and C. Chen, *J. Chem. Phys.* **105**, 10663 (1996).
- <sup>25</sup>E. V. Doktorov, I. A. Malkin, and V. I. Man'ko, *J. Mol. Spectrosc.* **64**, 302 (1977).
- <sup>26</sup>D. K. W. Mok, E. P. F. Lee, F.-T. Chau, and J. M. Dyke, *J. Chem. Phys.* **120**, 1292 (2004).
- <sup>27</sup>D. W. K. Mok, E. P. F. Lee, F.-t. Chau, and J. M. Dyke, *J. Chem. Theory Comput.* **5**, 565 (2009).
- <sup>28</sup>D. K. W. Mok, F.-T. Chau, E. P. F. Lee, and J. M. Dyke, *J. Comput. Chem.* **31**, 476 (2010).